Quantification of hydrogen uptake of steam-oxidized zirconium alloys by means of neutron radiography



2008 J. Phys.: Condens. Matter 20 104263

(http://iopscience.iop.org/0953-8984/20/10/104263)

IOP Publishing Journal of Physics: Condensed Matter

J. Phys.: Condens. Matter **20** (2008) 104263 (7pp) doi:10.1088/0953-8984/20/10/104263

# Quantification of hydrogen uptake of steam-oxidized zirconium alloys by means of neutron radiography

**M Grosse[1], G Kuehne[2], M Steinbrueck[1], E Lehmann[2], J Stuckert[1] and P Vontobel[2]**

[1] Forschungszentrum Karlsruhe, PO Box 3640, D-76021 Karlsruhe, Germany
[2] Paul Scherrer Institut Villigen, CH-5232 Villigen-PSI, Switzerland

E-mail: Mirco.Grosse@imf.fzk.de

Received 11 July 2007, in final form 14 November 2007
Published 19 February 2008
Online at stacks.iop.org/JPhysCM/20/104263

**Abstract**

The macroscopic total neutron cross section of zirconium alloys depends linearly on the hydrogen content in the metal. This offers the possibility of quantitative determination of the hydrogen content by means of neutron radiography. The method is applied to determine quantitatively the hydrogen content and distribution in corner rods of a VVER-type nuclear fuel bundle simulator investigated in the framework of post-test examinations of a large scale severe nuclear accident simulation experiment. Unexpectedly high hydrogen concentrations were found. The axial hydrogen distributions in the corner rods show two maxima. The reasons for these distributions and the large hydrogen content are not the temperature distribution but the appearance of oxide layers. Highest concentrations occur at positions where the oxide layers show a lot of open circumferential cracks. In these cracks large local hydrogen partial pressures can be expected. The hydrogen content at positions with compact oxide layers is much lower.

(Some figures in this article are in colour only in the electronic version)

## 1. Introduction

Loss of coolant accident (LOCA) scenarios are possible incidents in nuclear facilities such as nuclear power plants (Harrisburg, USA 1979) or spent nuclear fuel pools (Paks, Hungary 2003). In the framework of the QUENCH program of the Forschungszentrum Karlsruhe severe accident scenarios (accidents beyond the LOCA scenario) are studied. After the loss of coolant, the fuel rods become overheated. Reflooding of the reactor core as an accident management measure induces a strong production of water steam which oxidizes the hot fuel cladding in a strongly exothermic reaction:

$$2H_2O + Zr \Leftrightarrow ZrO_2 + 4H + 582\ \text{kJ mol}^{-1}\ (Zr). \quad (1)$$

As a result of this reaction free hydrogen is produced. The hydrogen may be released into the reactor environment, which leads to the risk of hydrogen detonation. Part of the hydrogen can be absorbed at least temporarily in the remaining zirconium of the cladding material by dissolution in the metal phase or as hydrides. This absorbed hydrogen temporarily affects the risk of hydrogen detonation and changes the time dependence of the hydrogen release during the scenario. A higher hydrogen content in the metal influences the $\alpha$–$\beta$-Zr phase composition and with it the solubility of oxygen in the metal. Also physical properties like the melting temperature depend on the metal phase composition. The absorbed hydrogen strongly affects the mechanical behaviour of the damaged fuel rod cladding, at least at low temperatures [1].

The aims of the large scale QUENCH experiments are the investigation of the hydrogen source term resulting from water injection into an uncovered core of a light-water reactor (LWR), the examination of the physico-chemical behaviour of overheated fuel elements under different flooding/cooling conditions, and the creation of a database for model verification, as well as development and improvement of severe fuel damage (SFD) computer codes. The QUENCH-12 experiment [2] was carried out to investigate the effects of core reflooding on the Russian-type VVER cladding materials (niobium-bearing Zr alloy E110) and bundle geometry.

 

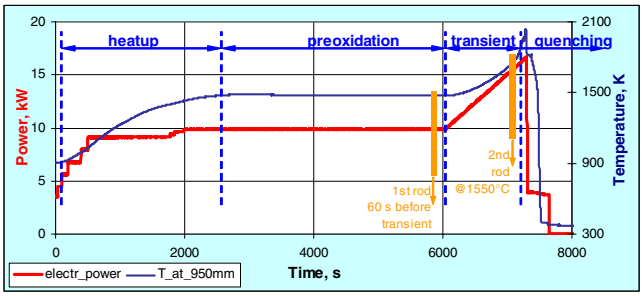


**Figure 1.** QUENCH-12 test summary with marks showing the corner rod withdrawals.

The post-test examinations include the determination of the absorbed hydrogen by means of neutron radiography.

Usually the hydrogen content in steam oxidized zirconium alloys is determined by measuring the composition of the off-gas during hot extraction. In former QUENCH experiments [3], with western-type pressurized water reactor (PWR) bundle simulators, it was found that between 0.8 and 6 at.% of the produced hydrogen is stored in the remaining metal. However, hot extraction is an integral and destructive method. It needs about 1–2 h annealing time per specimen and does not provide information about the hydrogen distribution in the specimen.

Alternatively, neutron radiography experiments provide the possibility of a fast, non-destructive, and quantitative determination of the hydrogen content with a spatial resolution better than 50 $\mu$m. Neutron radiography has been used in nuclear technique research for many years, e.g. for fuel rod inspections [4–9] or reactor thermo-hydraulic research [10]. In [5–7] the method is applied to analyse qualitatively the hydrogen distribution in nuclear fuel rods after service. Hydride lenses are found. In [8] neutron diffraction and radiography investigations are performed. A linear relationship between hydrogen concentration and a grey level in the neutron radiography image is found empirically in the radiography experiments. No physical basis of this relationship is specified. Unfortunately, no explicit information about transmissions and total cross sections of the samples are given. Therefore, the quantitative relations found in this paper are valid only for the used camera setup. They cannot be transferred to other experimental setups. However, the investigations demonstrate the capabilities of neutron radiography for the quantitative hydrogen determination with good spatial resolution.

In [9] hydrogen content in Zircaloy cladding tubes is determined quantitatively by neutron radiography and tomography. Here the relations between hydrogen concentration and a non background corrected transmission calculated from photo-stimulated image plate luminescence and computer tomography numbers, respectively, are given.

In our previous work the experimental setup was optimized and the calibration of the dependence of macroscopic total neutron cross section on hydrogen content was given [11]. The aim of this paper is to apply the method for quantitative determination of the axial hydrogen distribution in three corner rods of the QUENCH-12 experiment, withdrawn at three times during the experiment.

**Table 1.** Chemical composition of Zry-4 and E110; Zr balance.

| Alloy | Sn | Nb | Fe | Cr | O |
|---|---|---|---|---|---|
| Zry-4 | 1.50 | — | 0.21 | 0.10 | 0.14 |
| E110 | — | 0.97 | <0.01 | — | 0.05 |

## 2. QUENCH-12 experiment

The behaviour of a VVER bundle during reflooding was studied in the large scale QUENCH-12 experiment. The main phases in this test were pre-oxidation (53 min at 1473 K at the hottest axial position) and transient temperature increase with reflood and quenching (maximal temperature $\sim$ 2063 K). A schematic summary of the test phases is given in figure 1. In [2] the experiment is described in detail. The simulator claddings and the corner rod material were the original VVER-type Zr-1Nb alloy E110. The concentrations of the main alloying elements are given in table 1. In order to freeze the material state after certain phases of the experiment, corner rods were withdrawn. These corner rods allow us to examine the oxidation state and the hydrogen uptake at the time of withdrawal.

The first corner rod (D), which was taken at the end of the pre-oxidation phase, revealed an extensive breakaway effect in the oxide along the complete hot zone. The reason for this effect is mechanical stress caused from the tetragonal to monoclinic phase transition during growth of the zirconium oxide. It was not possible to measure the oxide layer thickness due to spalling of the oxide scales. The second rod (F) was withdrawn during the transient phase before starting the moderate temperature escalation. This rod also exhibited an extensive spalling of oxide scales. The third corner rod (B) was pulled after the test. Due to partial melting, this rod could not been withdrawn completely. An axial region of about $z$ = 880–1020 mm is lost by melt transport to the bottom. At the two remaining ends, deep holes in the middle of the rod cross sections were observed.

During the QUENCH experiment hydrogen in the off-gas is analysed by a state-of-the-art mass spectrometer, Balzers 'GAM300', located at the off-gas pipe about 2.70 m downstream of the test section. The time dependence of the hydrogen concentration in the off-gas measured by the mass spectrometer is plotted in figure 2. Until the end of the pre-oxidation phase about 34 g and during reflooding 24 g of hydrogen are released into the off-gas. The amount of hydrogen measured in the off-gas during the pre-oxidation phase is similar to the value measured for western-type PWR simulation bundles during the comparable test QUENCH-6 (32 g) with Zry-4 cladding and corner rod material. However, the release during reflooding for the VVER is a factor of six higher than for the PWR bundle (4 g).

## 3. Calibration of the correlation between total neutron cross section and hydrogen content

For calibration of the correlation between total macroscopic neutron cross section $\Sigma_{\text{total}}$ and hydrogen concentration,

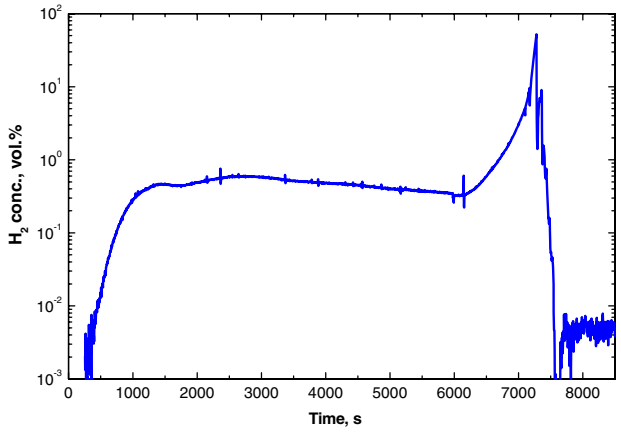


**Figure 2.** Time dependence of the hydrogen concentration in the off-gas.

cladding tube segments made from the Zr–Sn alloy Zircaloy-4 (Zry-4) were hydrogen loaded in $H_2$/Ar atmosphere at various temperatures between 1073 and 1373 K and hydrogen partial pressures of 10 and 50 kPa, resulting in H/Zr atomic ratios between 0.02 and 1.70. The length of the tube segments was 20 mm. The inner and outer diameters were $d_i = 9.25$ mm and $d_o = 10.75$ mm, respectively. The amounts of absorbed hydrogen were determined by measuring the specimen masses before and after annealing. According to Sieverts' law [12] different hydrogen concentrations in the specimens were reached.

The neutron radiographs were measured at the cold neutron radiography facility ICON at the SINQ neutron source (PSI, Switzerland) [13]. Figure 3 shows the radiographs of these calibration specimens together with the corresponding radial intensity distributions.

Horizontal intensity distributions were determined by quantitative analysis of the radiographs. The transmission $T$ of the neutron beam behind the specimen is given by:

$$T = \frac{I - I_B}{I_o - I_B} = \exp(-\Sigma_{total} s). \tag{2}$$

$I$ is the intensity behind the specimen, $I_0$ the primary beam intensity, $I_B$ the background intensity measured behind a Cd specimen with comparable dimensions and $s$ the path through the specimen. Due to hydrogen added to the Zry-4, $\Sigma_{total}$ can be given as:

$$N_H \sigma_{total,H} + \Sigma_{total,Zry-4} \tag{3}$$

where $\Sigma_{total,Zry-4}$ is the total macroscopic neutron cross section of the unhydrated Zry-4 specimen, $N_H$ the hydrogen atom number density and $\sigma_{total,H}$ the total microscopic cross section of hydrogen. For an illumination in a radial direction the path length $s$ through a tube shaped specimen is given by the complex equation:

$$s = \Re\left(\sqrt{d_o^2 - (x - x_0)^2} - \sqrt{d_i^2 - (x - x_0)^2}\right). \tag{4}$$

$\Re$ is the real part of the complex term, $x$ the actual radial position and $x_0$ the radial middle position of the specimen. For rod-shaped specimens, the second part of the real part is zero. The analysis of the measurements in the radial direction was performed by an averaging of the intensity in the $z$ direction over a height of 10 mm. Due to this height, the intensity fit at the sample edges is very sensitive for the sample alignment, whereas the middle ranges are not influenced strongly. Therefore for the analysis only the middle positions were used where:

$$s \approx d_o - d_i \tag{5a}$$

and

$$s \approx d_o \tag{5b}$$

for cladding tube segments and for the rods, respectively. The total cross sections of the calibration specimens were calculated according to (2) and (5*a*). $\Sigma_{total}$ increases strongly with increasing hydrogen content. The good agreement between measured data and fit given in figure 4 proves the linear dependence of the total cross section on the atomic ratio, at least for H/Zr < 0.8:

$$\Sigma_{total} = \left(0.21 + 2.90\frac{H}{Zr}\right) \text{ cm}^{-1}. \tag{6}$$

A detailed description of the calibration, including a comparison of measurements with cold and thermal neutrons and with and without a beryllium filter as well as a discussion of the influence of $ZrO_2$ layers, is given in [11].

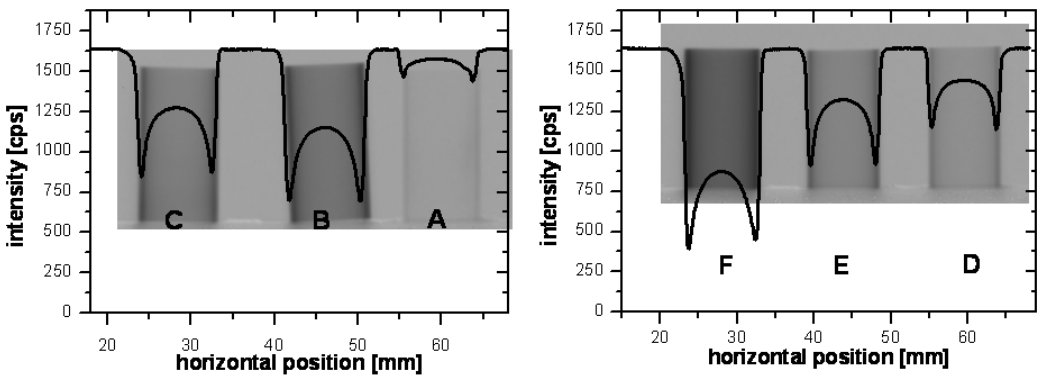


**Figure 3.** Neutron radiography image and horizontal intensity distribution of the hydrogen loaded calibration specimens.

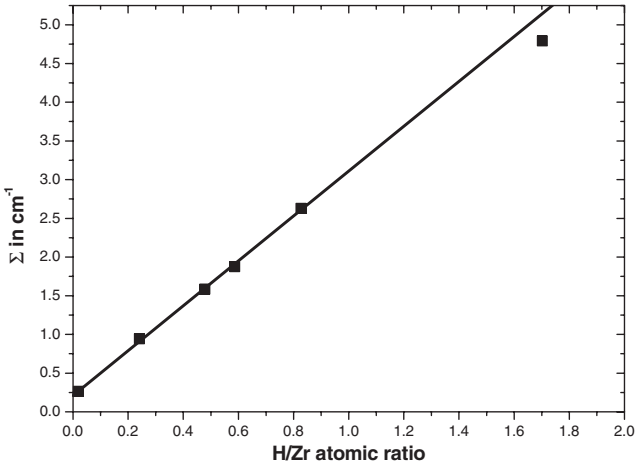


**Figure 4.** Correlation between the H/Zr atomic ratio and total neutron cross section.

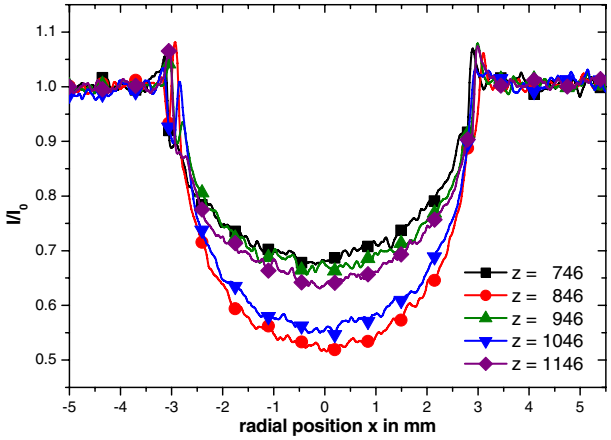


**Figure 5.** Normalized radial intensity distribution of five axial positions of corner rod D (each 50th point is marked with a symbol).

## 4. Measurement of the hydrogen concentration in QUENCH-12 corner rods

The method was applied to analyse the hydrogen stored in the corner rods of the QUENCH-12 bundle. The measurements were performed at the cold neutron radiography facility ICON (SINQ, PSI, Switzerland) with a camera length $L/d$ of 350. $L$ is the aperture to sample distance and $d$ the aperture opening size.

The neutron radiographs were detected by a camera system, specially developed for neutron micro-tomography applications. It consists of an ultra-thin Gadox scintillator (thickness 10 $\mu$m), a lens without any optical distortions (diameter: 155 mm, height: 620 mm mass: 30 kg) and the high resolution 1:1 magnification CCD camera ANDOR DV436 (Peltier cooled, pixel size 13.5 $\mu$m, field of view: 28 mm × 28 mm, 2048 × 2048 pixels, 16 bit).

The data were analysed with the 'ImageJ' software package. The measurements were normalized with an open beam frame and corrected for dark current. With an axial step size of 20 mm the intensity distribution of the position perpendicular to the rod axis was determined by integration over an axial width of 1 mm. The background intensity found behind a Cd specimen of comparable size was subtracted.

## 5. Results and discussion

The result of the calibration measurements given in figure 4 confirms that the linear dependence of the total macroscopic neutron cross section on hydrogen content in the zirconium alloy behaves as to be expected from equation (3). The neutron transmission decreases exponentially with increasing hydrogen content for a certain neutron wavelength. The path through the specimens is small enough that beam hardening effects can be neglected. For this reason the exponential decay is also valid for radiography experiments with a broader neutron spectrum. It is in contrast to the result given in [8]. Here a linear dependence of the neutron transmission on the hydrogen content is reported. According to (2) the grey level which is a measure for neutron transmission should depend exponentially on hydrogen concentration. The dependence is only approximately linear for low concentrations.

The neutron transmission of the QUENCH-12 corner rods strongly depends on the axial position. As an example, normalized radial intensity distributions are given in figure 5 for five axial positions. At the two edges of the regions behind the rod small increases of the intensities are visible. This increase is caused by Fraunhofer diffraction. In the region attenuated by the rods the intensity distribution can be described by equations (2) and (5*b*). It is a hint that no radial gradients in the hydrogen distribution exist. Since the total macroscopic cross section of hydrogen free E110 alloy is very close to the cross section of hydrogen free Zry-4, the H/Zr atomic ratio can be determined according to (6). From this ratio the hydrogen content $c_{\mathrm{H}}^{m}$ in at.% is given by:

$$c_{\mathrm{H}}^{m} = 100\frac{\mathrm{H}}{\mathrm{Zr}}\Big/\left(1+\frac{\mathrm{H}}{\mathrm{Zr}}\right). \tag{7}$$

The obtained axial distribution of the hydrogen content in the three investigated corner rods determined by (6) and (7) is shown in figure 6. The absolute values are much higher than those found for the comparable QUENCH-6 experiment with western-type PWR simulator rod configuration and Zry-4 cladding and corner rod material (one broad maximum in the axial distribution, maximal hydrogen content about 10 at.%). From the results it can be roughly estimated that one quarter of the free hydrogen produced in the pre-oxidation phase of the QUENCH-12 experiment is absorbed in the zirconium alloy.

The unexpectedly high hydrogen release during reflooding, additional to the free hydrogen production by the strong oxidation, can be explained by an immediate desorption of the hydrogen taken up before.

A large amount of the thin cladding tubes was oxidized. Due to the very low hydrogen solubility in $ZrO_2$, H is desorbed from the claddings to the gas environment.

For rod D two local maxima at $z \approx 850$ and 1080 mm and a local minimum at $z \approx 970$ mm was found. The axial positions of these extrema are the same for rod F but the

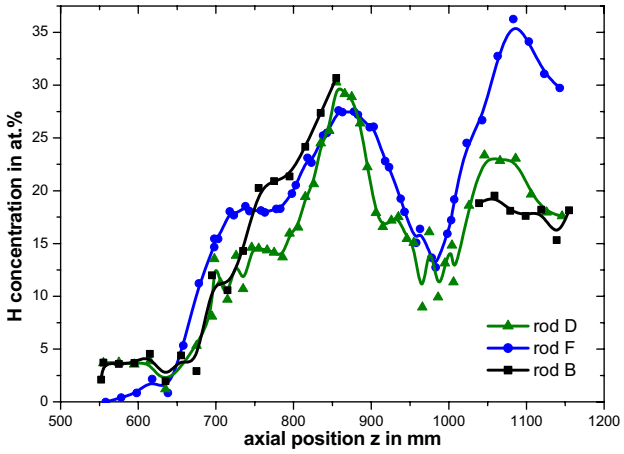


**Figure 6.** Axial distribution of the hydrogen content for the three investigated corner rods.

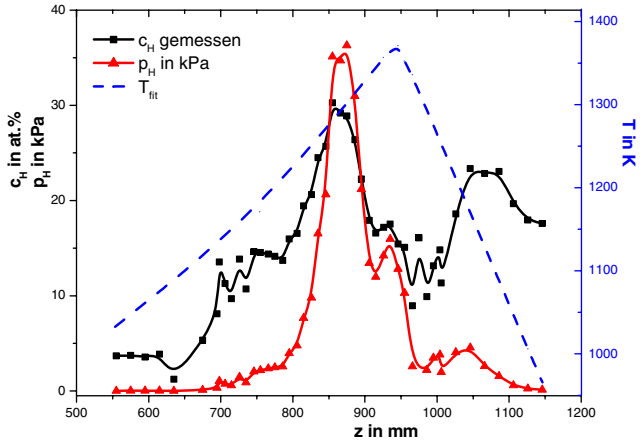


**Figure 7.** Fit of axial temperature distribution, determined hydrogen content, and calculated hydrogen partial pressure for corner rod D.

maximum at 1080 mm is significantly higher than for rod D. The second maximum in rod B is very flat. The minimum would be in the region lost by melting.

The analysis of the axial hydrogen distributions has to be focused at first on the discussion of the results for corner rod D. This rod is withdrawn after 53 min isothermal pre-oxidation at 1473 K (at centre rod, $z = 950$ mm). Due to the large time and the relatively high temperatures, a quasi-equilibrium state can be assumed. The chemical reaction given in (1) shows at temperatures higher than 1273 K a parabolic kinetics. The changes in the free hydrogen production rate are low after long times (see figure 2). Due to the breakaway effect at temperatures between 1073 and 1273 K the steam oxidation kinetics is linear. For the axial regions having this temperature range the free hydrogen production rate is constant. It means that according to Sieverts' law an equilibrium between the hydrogen in the gas phase and in the metal has to be established, independently of the oxide layer between these two phases:

$$c_{\mathrm{H}}^{m} = k_{\mathrm{s}}\sqrt{p_{\mathrm{H}}} \tag{8}$$

where $k_{\mathrm{s}}$ is the Sievert constant and $p_{\mathrm{H}}$ the hydrogen partial pressure in the gas. In [12] the temperature dependence of $k_{\mathrm{s}}$ is determined also for E110. The axial temperature distribution can be fitted by two lines given in figure 7. From the axial temperature and hydrogen concentration distributions the axial hydrogen partial pressure distribution can be calculated according to equation (8).

The distribution of the hydrogen partial pressure reaches a maximum at $z \approx 870$ mm, as figure 7 shows. The estimated maximal value of $p_{\mathrm{H}} \approx 36$ kPa is two orders of magnitude higher than the hydrogen partial pressure in the off-gas at the time of withdrawing rod D determined by mass spectrometry (figure 2). Such a high H partial pressure in the bulk of the gas phase can be excluded because the oxidation behaviour gives no hint that such a strong reaction is needed to produce this high partial pressure. However, for the equilibrium, not the gas bulk hydrogen concentration but the gas hydrogen partial pressure at the rod surface is important. In figure 8 the optical

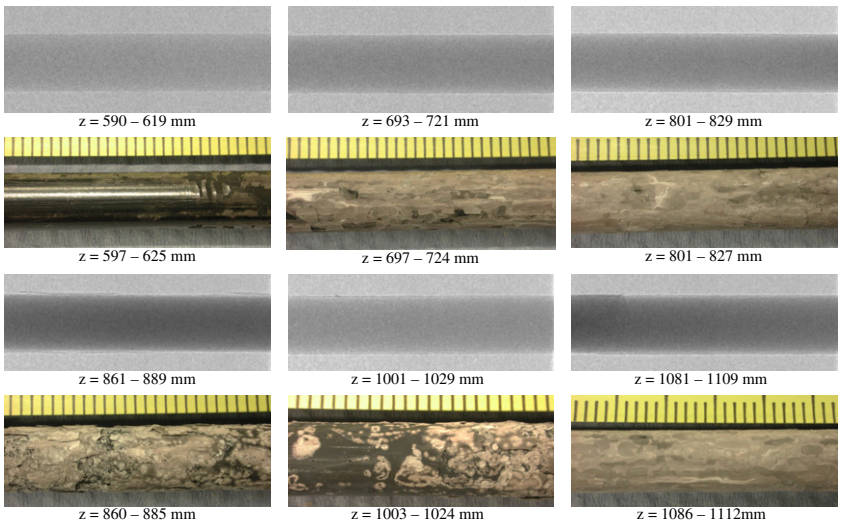


**Figure 8.** Neutron radiographs and optical appearance of typical axial positions of corner rod D.

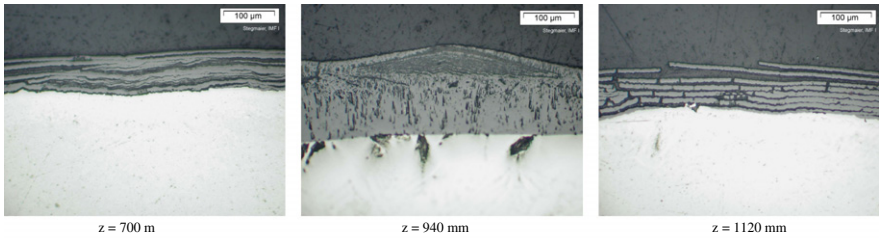


**Figure 9.** Micrographs of parts of the cross sections at different axial positions of corner rod D.

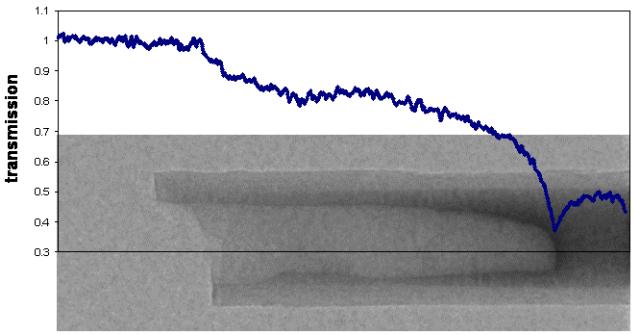


**Figure 10.** Neutron radiograph of the upper end of the lower part of corner rod B ($x$ axis is the position of the transmission graph).

oxide layer appearance and neutron radiographs are given. A comparison of the images shows that the highest hydrogen content can be found at positions with a thick oxide scale containing large open cracks clearly visible in the micrographs. Figure 9 shows typical micrographs of cross sections at axial positions $z = 700$ mm (beginning of the first hydrogen peak), $z = 940$ mm (location of the local minimum of the H concentration), and $z = 1120$ mm (position in the range of the second peak). Steam can penetrate into these cracks. The remaining oxide barrier between the crack front and the metal is small or the crack grows directly into the metal. Therefore a relatively strong oxidation occurs at crack positions. The release of the gases out of the crack is small. Consequently, hydrogen is here strongly enriched.

The quasi-equilibrium model cannot be applied to discuss the hydrogen content and distribution in rods F and B, withdrawn during and after the transient phase, respectively. For instance, the equilibrium hydrogen partial pressure at $z = 1080$ mm in rod F would be about 450 kPa. Such a high pressure would destroy the oxide layer. Obviously, the hydrogen has not enough time to diffuse out of the corner rod bulk.

The neutron radiograph of the upper end of the lower part of rod B is shown in figure 10. It is comparable to the lower end of the upper part of this rod. The deep hole is clearly visible. At the hole surface the dark grey colour indicates a high hydrogen content (see graph of the axial variation of the neutron transmission). The formation of these holes can be explained by the $\alpha$–$\beta$ phase composition. At the high temperatures at the beginning of the reflood the bcc $\beta$ phase is thermodynamically stable. However, dissolved hydrogen stabilizes this phase, but absorbed oxygen stabilizes the hexagonal $\alpha$ phase. During the transient reflooding, hydrogen diffuses from the rod surface into the gas environment whereas oxygen diffuses into the metal. The $\alpha$ phase at the outer regions and $\beta$ phase in the bulk of the rod are established. Due to the lower melting temperature of the $\beta$ phase (2128 K) than of the oxygen stabilized $\alpha$ phase (2248 K) a partial melting of the bulk occurs whereas the outer regions remain solid. After solidification, stresses and micro-cracks can be formed at the interface and the rod breaks along this interface.

## 6. Summary and conclusions

The investigations show that neutron radiography is a powerful tool for the analysis of hydrogen in zirconium alloys. The method provides the possibility of a fast, quantitative, and non-destructive determination of hydrogen with a spatial resolution of about 50 $\mu$m.

A linear dependence of the total neutron cross section on the H/Zr atomic ratio was determined. The results of the analysis of the hydrogen concentration and distribution in the QUENCH-12 corner rods show that hydrogen is accumulated in the remaining metallic Zr alloys during the pre-oxidation phase. During temperature rise at the beginning of the reflooding phase a large amount of hydrogen absorbed in the metal is released at once in addition to the free hydrogen produced by the strong oxidation. A short but very high hydrogen peak is the consequence. The hydrogen uptake of the zirconium alloy E110 is mainly determined by very local gas conditions at the metal or oxide surface. These conditions are strongly influenced by the macroscopic oxide appearance. This fact is not yet taken into account in computer codes simulating severe accidents. Models considering the hydrogen absorption (at least in some effective way) have to be included in such SFD computer codes [14, 15] to describe the severe accident behaviour of VVER-type reactors well.

## Acknowledgments

This work is based on experiments performed at the ICON facility of the Swiss spallation neutron source SINQ, PSI, Villigen, Switzerland. The authors thank G Frei, from PSI-ASQ for his support during the radiography experiments and U Stegmaier and P Severloh from FZK-IMF1 for the metallographic investigations.

## References


[1] Kim J H, Lee M H, Choi B K and Jeong Y H 2005 *Nucl. Engin. Design* **235** 67

[2] Stuckert J, Sepold L and Steinbrueck M 2007 Results of the QUENCH-12 reflood experiment with a VVER-type bundle ICONE-15: *Proc. 15th Int. Conf. on Nuclear Engineering (Nagoya, 2007)* CD-ROM PaperICONE-15-10257

[3] Sepold L, Hofmann P, Leiling W, Miassoedov A, Piel D, Schmidt L and Steinbrueck M 2001 *Nucl. Eng. Des.* **204** 205

[4] Bastürk M, Tatlisu H and Böck H 2006 *J. Nucl. Mater.* **350** 240

[5] Lehmann E, Vontobel P and Hermann A 2003 *Nucl. Instrum. Methods* A **515** 745

[6] Lehmann E, Vontobel P and Kardjilov N 2004 *Appl. Radiat. Isot.* **61** 503

[7] Gröschel F, Schleuniger P, Hermann A and Lehmann E 1999 *Nucl. Instrum. Methods* A **424** 215

[8] Svab E, Meszaros G, Somogyvari Z, Balasko M and Körösi F 2004 *Appl. Radiat. Isot.* **61** 471

[9] Yasuda R, Matsubayashi M, Nakata M and Harada K 2002 *J. Nucl. Mater.* **302** 156

[10] Harvel G D, Chang J S and Krishnan V S 2000 *Nucl. Eng. Des.* **200** 221

[11] Grosse M, Lehmann E, Vontobel P and Steinbrueck M 2006 *Nucl. Instrum. Methods Phys. Res.* A **566** 739

[12] Steinbrueck M 2004 *J. Nucl. Mater.* **334** 58

[13] Kühne G, Frei G, Lehmann E and Vontobel P 2005 *Nucl. Instrum. Methods* A **542** 264

[14] Repetto G, De Luze O, Birchley J, Drath T, Hollands T, Koch M K, Bals C, Trambauer K and Austregesilo H 2007 Preliminary analyses of the Phebus FPT3 experiment using Severe Accident Codes (ATHLET–CD, ICARE/CATHARE, MELCOR) *ERMSAR-2007: 2nd European Review Meeting on Severe Accident Research (Karlsruhe, June 2007)*

[15] Kleinhietpass I and Koch M 2003 *atw* **48** 762